



Munich Personal RePEc Archive

Catalytic thermal degradation of Chlorella Vulgaris: Evolving deep neural networks for optimization

Teng, Sin Yong and Loy, Adrian Chun Minh and Leong, Wei Dong and How, Bing Shen and Chin, Bridgid Lai Fui and Máša, Vítězslav

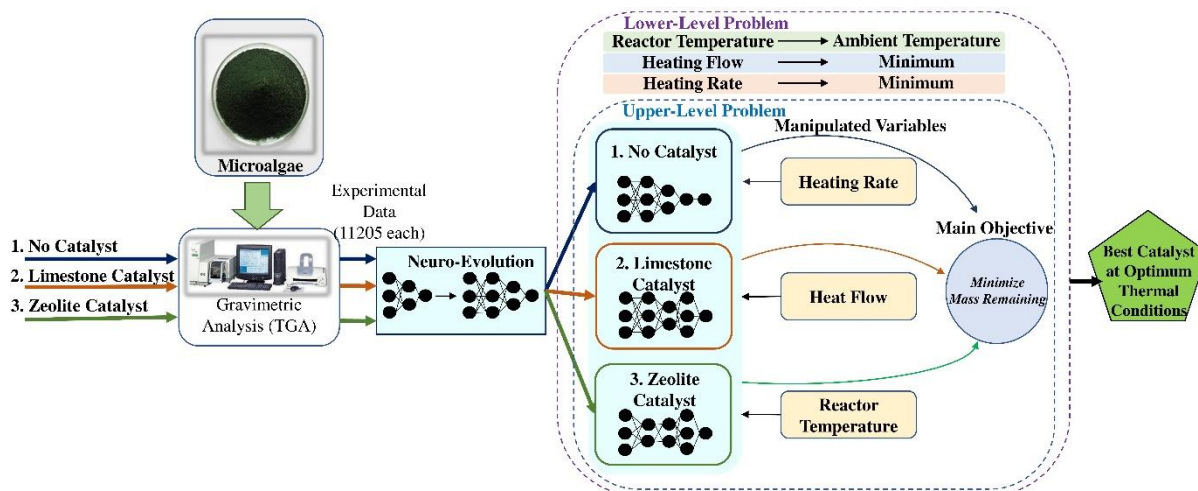
Brno University of Technology, Institute of Process Engineering
NETME Centre, Technicka 2896/2, 616 69 Brno, Czech Republic,
National HiCoE Thermochemical Conversion of Biomass, Centre for
Biofuel and Biochemical Research, Institute of Sustainable Building,
Chemical Engineering Department, Universiti Teknologi
PETRONAS, Seri Iskandar, Perak 32610, Malaysia, Department of
Chemical and Environmental Engineering, University of Nottingham
Malaysia Campus, Jalan Broga, 43500 Semenyih, Selangor,
Malaysia, Chemical Engineering Department, Faculty of
Engineering, Computing and Science, Swinburne University of
Technology, Jalan Simpang Tiga, 93350 Kuching, Sarawak,
Malaysia, Department of Chemical Engineering, Faculty of
Engineering and Science, Curtin University Malaysia, CDT 250,

98009 Miri, Sarawak Malaysia

19 September 2019

Online at <https://mpra.ub.uni-muenchen.de/95772/>
MPRA Paper No. 95772, posted 19 Oct 2019 15:07 UTC

Graphical Abstract



This work was published at Bioresource Technology

Please cite the work if it has been useful to you. The article can be cited as:

Teng, S.Y., Loy, A.C.M., Leong, W.D., How, B.S., Chin, B.L.F., and Máša, V. (2019). Catalytic Thermal Degradation of *Chlorella Vulgaris*: Evolving Deep Neural Networks for Optimization. Bioresource Technology. doi:10.1016/j.biortech.2019.121971

Highlights

- Thermal behavior of *C. vulgaris* were analyzed.
- Effects of the presence of limestone and HZSM-5 zeolite catalysts were investigated.
- Novel PDSE neuro-evolution algorithm was proposed for neural architecture search.
- Neuro-evolution achieved RMSE of 0.005-0.007, considered state-of-art for TGA studies.
- Simulated Annealing was used in optimization of operating conditions of the pyrolysis.

Catalytic Thermal Degradation of *Chlorella Vulgaris*: Evolving Deep Neural Networks for Optimization

Sin Yong Teng^{a,#}, Adrian Chun Minh Loy^{b,#}, Wei Dong Leong^c, Bing Shen How^{d,*}, Bridgid Lai Fui Chin^e, Vítězslav Máša^a

^aBrno University of Technology, Institute of Process Engineering & NETME Centre, Technická 2896/2, 616 69 Brno, Czech Republic.

^bNational HiCoE Thermochemical Conversion of Biomass, Centre for Biofuel and Biochemical Research, Institute of Sustainable Building, Chemical Engineering Department, Universiti Teknologi PETRONAS, Seri Iskandar, Perak 32610, Malaysia.

^cDepartment of Chemical and Environmental Engineering, University of Nottingham Malaysia Campus, Jalan Broga, 43500 Semenyih, Selangor, Malaysia.

^dSwinburne University of Technology Sarawak Campus, Jalan Simpang Tiga, 93350 Kuching, Sarawak, Malaysia.

^eDepartment of Chemical Engineering, Faculty of Engineering & Science, Curtin University, Sarawak Campus, CDT 250, 98009 Miri, Sarawak, Malaysia.

*Corresponding Author: bshow@swinburne.edu.my

#Author contributed equally to this work

Abstract

The aim of this study is to identify the optimum thermal conversion of *Chlorella Vulgaris* with neuro-evolutionary approach. A Progressive Depth Swarm-Evolution (PDSE) neuro-evolutionary approach is proposed to model the Thermogravimetric analysis (TGA) data of Catalytic Thermal Degradation of *Chlorella Vulgaris*. Results showed that the proposed method can generate predictions which are more accurate compared to other conventional approaches (> 90 % lower in Root Mean Square Error (RMSE) and Mean Bias Error (MBE)). In addition, Simulated Annealing is proposed to determine the optimal operating conditions for microalgae conversion from multiple trained ANN. The predicted optimum conditions were reaction temperature of 900.0 °C, heating rate of 5.0 °C/min with the presence of HZSM-5 zeolite catalyst to obtain 88.3 % of *Chlorella Vulgaris* conversion.

Keywords

Microalgae, Thermogravimetric Analysis, Artificial Neuron Network, Particle Swarm Optimization, Simulated Annealing

1. Introduction

The global demand of energy supply is increasing rapidly due to population and economic growth (OPEC, 2019). In 2018, the global energy demand has an exceptional growth rate of 2.3 % which was further resulting in a 1.7 % increment of global carbon emissions (IEA, 2019). This strikes a challenge to achieve a balance between global warming and sustainable energy supply. Thus, many

countries around the world are seeking for alternative options to reduce the dependency on fossil fuel (Adenle et al., 2013).

Biofuel is a potential energy source that can be used as an alternative to fossil fuel (Milano et al., 2016). In the last decades, the third generation (3G) biofuel which is derived from microalgae have received great attention since first generation (1G) and second generation (2G) biofuels contain food security issue (Mohr and Raman, 2013) and sustainability concern (Sun et al., 2019) respectively. In general, the main advantages of using microalgae as biofuel production feedstock encompasses of easy cultivation; higher growth rates and productivity; attractive oil yield; and lower carbon emissions (Mata et al., 2010; Costa and Morais, 2011).

Among the various technologies established for converting microalgae to biofuels (e.g., pyrolysis, hydrothermal carbonization, and gasification (Chan et al., 2019)), catalytic pyrolysis is one of the most preferable technologies (Zainan et al., 2018). A series of catalysts have been studied thoroughly on their ability to break large hydrocarbon aromatic compounds of biomass into smaller hydrocarbon compound via decarboxylation (Mettler et al., 2014), dehydration (Barnard and Hughes, 1960) and deoxygenation (Raymundo et al., 2019) reactions. Among all the catalysts, HZSM-5 zeolite and CaO catalysts have driven more attention due to their performance in upgrading the bio-oil quality and enhance the yield of bio-oil (Zhang et al., 2019). HZSM-5 zeolite is highly selective for aromatics and effective in deoxygenation of oxygenated compounds to form olefins and phenolics (Yang et al., 2018). Meanwhile, CaO has been introduced into pyrolysis process as an alkali metal oxide catalyst. It is normally extracted from limestone and eggshell waste due to highly abundant, high CaO composition, and relatively low cost (Gan et al., 2018).

Thermogravimetric analysis (TGA) is used to investigate the thermal degradation of biomass by measuring the rate of weight loss as a function of temperature and time. Gai et al. (2013) had investigated the kinetic parameters of *Chlorella pyrenoidosa* (CP) and *Spirulina plantensis* (SP) microalgae. They reported the average activation energy of CP and SP were 77.02 and 91.56 kJ/mol. Besides, Kim et al. (2012) reported on the lumped kinetic model using *Saccharina Japonica* as feedstock. The average activation energy obtained was in the range of 102.5-269.7 kJ/mol. Most works are focusing on the kinetic parameters of the chemical mechanism of the thermal decomposition of microalgae. There is still limited literature on the optimization study on the mass loss percentage (MLP) of thermal degradation of biomass.

Artificial neural network (ANN) have been recently applied to model the thermochemical performances of biomass pyrolysis due to its credibility in addressing complex nonlinear problems. In the early of 21st century, Abbas et al. (2003) had proposed the use of neural network model in predicting the devolatilization performances of coal and biomass. The computing efficiency of the model was proven to be more attractive compared to other existing tools Conesa et al. (2004) then developed a predictive model using a multilayer ANN, to estimate the thermal decomposition of cellulose, lignin and polyethylene. This research has been extended to study the thermochemical performance of various feedstocks via pyrolysis (e.g., keratin biopolymer (Fazilat et al., 2012); sewage sludge (Naqvi et al., 2018), etc.). The popularization of ANN being used to analyze experiments datasets from TGA systems is mainly due to (i) the large size of the datasets from TGA systems (> 10,000 data per run); (ii) the complex non-linear nature of thermal conversion

that requires advanced analytics for prediction and modeling; (iii) fully automatic modeling procedure that can be achieved by ANN.

Conventional practices in training neural network for the application of TGA analysis considers single-hidden layer neural networks (Abbas et al., 2003). Although researchers acknowledge that the consideration of better hyperparameters for ANN is important in TGA analysis (Mayol et al., 2018), hyperparameter optimization is rarely carried out for the applications of thermal analysis. Besides, the current norm for researchers is to use trial and error methods to find an acceptable ANN topology. This is demonstrated in a recent work of Naqvi et al. (2018), which tested neural network with lesser than 3 hidden layers. Nevertheless, Mhaskar and Poggio (2016) highlighted the importance of deeper networks from an approximation theory perspective. Another issue is on the activation functions of ANN, commonly one or only a few types (Mayol et al., 2018) of activation function are considered by trial and error for the application of TGA. From a computational intelligence perspective, a good methodology to achieve optimality instead of trial-and-error is by using Neuro-evolution (Stanley and Miikkulainen, 2002). This method is very popular in the fields of Deep Learning because natural brains themselves are the products of bio-evolutionary processes, and its implementation enables large-scale computing (Stanley et al., 2019). Based on the results obtained by the researchers from Deep Mind (Jaderberg et al., 2017) and OpenAI (Salimans et al., 2017), it can be confirmed that Neuro-evolution is highly effective and implementable even when considering computational scalability.

To-date, none of the work has utilized this approach for the purpose of TGA thermal analysis. Thus, the objective of this work is to incorporate the use of Neuro-evolutionary approach in the applications of analyzing TGA experimentation data. The increase in accuracy of the neural network prediction has allowed for a more indicative optimization study on the ANN model. However, the optimization study was not performed in the previous works (e.g., Naqvi et al. (2018) and Conesa et al. (2004)) mainly due to the complex structure of ANN, which makes conventional optimization strategies non-straightforward. To address this issue, this work proposes the use of Simulated Annealing (Metropolis et al., 1953), a metaheuristic algorithm, to search for the optimal thermal conditions for microalgae conversion from multiple trained ANN.

2. Materials and methods

2.1 Experimental description

The microalgae biomass *Chlorella vulgaris* (*C. vulgaris*) was obtained from Centre for Biofuel and Biochemical, Universiti Teknologi PETRONAS (UTP), Malaysia. The biomass was dried and sieved to a particle size less than 200 μm . Moreover, limestone and HZSM-5 zeolite catalysts were obtained from Calrock Sdn. Bhd. and Sigma-Aldrich, Malaysia, respectively. Both catalysts undergo pre-treatment such as the limestone was heated at temperature 900.0 $^{\circ}\text{C}$ for 4 hours to ensure all the CaCO_3 in limestone was fully converted to CaO whereas HZSM-5 zeolite catalyst was calcined at 550.0 $^{\circ}\text{C}$ for 3 hours to activate the Bronsted acid sites. After that, the *C. vulgaris* samples were analyzed using thermogravimetric analyzer (TGA-DSC 1, Mettler Toledo) and LECO CHNS-932 elemental analyzer, respectively to determine the physical and chemical

properties of the samples. From the ultimate analysis of *C. vulgaris*, the carbon, hydrogen, nitrogen, sulphur and oxygen contents were 42.6 wt%, 8.2 wt%, 1.3 wt%, 0.8 wt% and 47.1 wt%, respectively. Whereas, the moisture, volatile matter, fixed carbon and ash content of *C. vulgaris* showed in the proximate analysis were 8.3 wt%, 59.2 wt%, 15.8 wt% and 16.7 wt%, respectively.

The pyrolysis studies were performed using five different heating rates of 10, 20, 30, 50 and 100 °C/min, respectively using the TGA equipment. Firstly, 100 ml/min of nitrogen gas (N₂) supply was introduced into the TGA for 10 min to avoid unwanted oxidation reaction of the biomass sample. After that, 10 mg of *C. vulgaris* biomass was introduced into the TGA and heated from 50.0 °C to 900.0 °C under non-isothermal conditions. Meanwhile, for catalytic pyrolysis process, the catalyst (e.g. limestone and HZSM-5 zeolite) with a ratio of 1:10 to the biomass was mixed homogenous with the *C. vulgaris* and loaded into the system. All experiments were carried out three times to ensure the reliability of the results.

2.2 Neural network generation

The experimentation data consists of heating rate (°C/min), heat flow (mW) and reactor temperature (°C) while providing results on the mass of microalgae remaining after the reaction. Three cases of experimentation were carried out which is the case with no catalyst, with limestone catalyst and HZSM-5 zeolite catalyst. The three separate datasets each containing 11,205 data points, giving a total of 33,615 data points. Each dataset was split with a ratio of 8:2 for training and validation. The ANN that was considered in this work is a fully connected neural network with a variable depth as shown in Fig. 1.

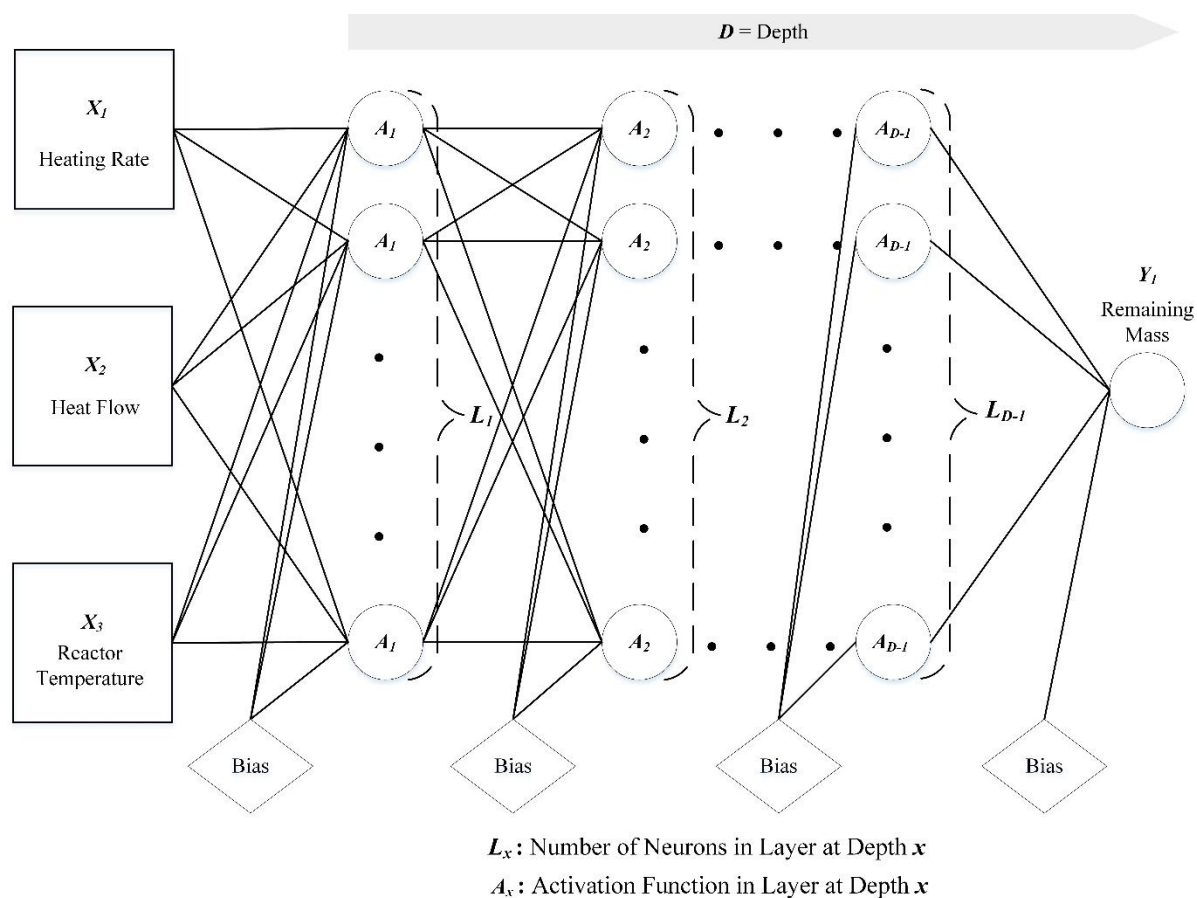


Fig. 1: Structure of fully connected neural network with variable depth considered.

From Ding et al. (2011), neuro-evolutionary strategies can be applied on the weights of ANN, architecture of ANN, and the activation function of ANN. However, due to the formulation of ANN being mathematically differentiable, the use of stochastic gradient descent (SGD) algorithms such as Adam (Kingma and Ba, 2014) is more suitable to be used on directly training the weights of ANN (Stanley et al., 2019) as it can utilize the gradient of the ANN for more efficient weight updates. Contrarily, the search for neural architecture and activation functions can be learned using Neuro-evolution approaches on top of SGD-based weight training (Floreano et al., 2008).

Considering the computational costs of Neuro-evolution algorithms, this paper proposes an algorithm called Progressive Depth Swarm-Evolution (PDSE) that is based on the efficient and robust modified Particle Swarm Optimization (PSO) algorithm (Shi and Eberhart, 1998). PDSE uses a variable length embedding for the population by progressively searching from shallow neural networks to deeper neural networks. Furthermore, the computational costs of this neuro-evolution algorithm can be effectively bounded by allocating a maximum search cost for each number of depths of ANN. The details of the algorithm are presented as pseudocode in Fig. 2

Progressive Depth Swarm-Evolution (PDSE) for Evolving Neural Networks

```

1: For  $i$  in  $C$  •  $C$  is datasets, which is type of catalyst in this case
2:   For  $j$  in  $D$ ,  $D = [D_L, D_h]$  •  $D$  is depth of neural network, which is bounded by a range
3:    $M \leftarrow$  Maximum Search Cost;  $DepthBest \leftarrow 1$ 
4:   Architecture  $\leftarrow$  List of size  $D$ ; Activation  $\leftarrow$  List of size  $D$ 
5:    $P \leftarrow$  Concatenate  $[D, \text{Architecture}, \text{Activation}]$  • Create encoded population,  $P$ 
6:    $v \leftarrow$  Randomize with size  $P$  • Initialize velocity,  $v$  which corresponds to  $P$ 
7:   While Networks Evaluated  $< M$ 
8:      $F \leftarrow$  Evaluate Network( $P$ ) • Train population of ANN according to population and get fitness,  $F$ 
9:      $v \leftarrow w v + \phi_p \text{rand}_p(\text{LocalBest}-P) + \phi_g \text{rand}_g(\text{GlobalBest}-P)$  • Update velocity by PSO
10:     $P \leftarrow P + v$  • Update position by PSO
11:    If GlobalBest  $< DepthBest$ :
12:       $DepthBest \leftarrow GlobalBest$  • Update best neural topology for the depth

```

Fig. 2: Pseudo-code for Novel Progressive Depth Swarm-Evolution (PDSE)

In this work, a particle-to-generation ratio of 2:5 and maximum search cost of 1000 were used. The PSO algorithm is extended from the EvoOpt library (Teng, 2019). For this application, the PDSE algorithm was used to search for ANN of depth 2 to 10 with fitness set to its validation loss. For the training of the weights in ANN, the popular stochastic gradient descent-based algorithm, Adam was used with batch size of 128 (Kingma and Ba, 2014). To prevent overfitting of the ANN, early stopping technique was implemented with a setting of minimum delta of 0.0001 and patience of 3.

The metric that is being used for training (loss) is the Mean Squared Error (MAE) as it provides a globally differentiable loss function for smooth training. For the purpose of benchmarking, 3 additional metrics were used, which are Root Mean Squared Error (RMSE), Mean Bias Error (MBE) and the coefficient of determination (R^2):

$$RMSE = \sqrt{\frac{\sum_{t=1}^N (\hat{y}_t - y_t)^2}{N}} \quad (1)$$

$$MSE = \frac{\sum_{t=1}^N (\hat{y}_t - y_t)^2}{N} \quad (2)$$

$$MBE = \frac{\sum_{t=1}^N (\hat{y}_t - y_t)}{N} \quad (3)$$

$$R^2 = 1 - \frac{\sum_{t=1}^N (\hat{y}_t - y_t)^2}{\sum_{t=1}^N (y_t - \bar{y})^2} \quad (4)$$

where y_t is actual data, \hat{y}_t is predicted data, \bar{y} is the mean of actual data, while N is the total number of actual data.

2.3 Bi-layer optimization

ANN serves as a good predictive regression tool. However, an optimization tool has to be deployed on the black-box ANN in order to find the predicted optimal thermal conditions and the most suitable catalyst of thermal degradation of microalgae. This work formulates this optimization problem into a bi-level optimization problem, where the main problem is to minimize the mass of the remaining microalgae after the reaction, Y_1 enabling efficient conversion. The outer problem is to minimize the conditions of the reaction to standard conditions and achieve better energy efficiency. The formulation of this bi-level optimization problem is shown in Eqs. (4) and (5):

min Y_1

$$\text{Subject to } X_{i,L} \leq X_i \leq X_{i,H} \quad \forall i \in 1,2,3 \quad (4)$$

min $|X_1| + |X_2| + |X_3 - T_{ambient}|$

$$\text{Subject to } X_{i,L} \leq X_i \leq X_{i,H} \cap Y_1 = Y_1^* \quad \forall i \in 1,2,3 \quad (5)$$

where X_1 , X_2 , X_3 are the rate of change in temperature, heat flow and the reactor temperature respectively. Y_1^* is the optimal mass of remaining microalgae from the main problem. For this work, the constraints used are 5.0 to 100.0 °C/min for X_1 , 0.0 mW to 300.0 mW for X_2 , and a varying range of 50.0 °C interval for X_3 . The ambient temperature is taken as 25.0 °C.

In order to solve the optimization problem, this work uses Simulated Annealing, which is a stable and well-known metaheuristics algorithm. The choice of this metaheuristic algorithm is due to Simulated Annealing being able to find global optimum points by escaping local minima and guarantees statistically robust results in short computation time (Goffe et al., 1994). The advantages of Simulated Annealing are particularly useful for this application, where the trained ANN is found to have multiple minimum points and a complex surface. The Simulated Annealing algorithm has its inspiration from metallurgical annealing, which involves heating and cooling of material to reduce their defects. This algorithm can be presented in five simple steps:

Step 1: Generate initial solution randomly.

Step 2: Find a neighbor solution for each of the initial solutions.

Step 3: Stochastically choose a solution between the initial and neighbour solution based on the probability, $p = \exp(-(\text{Fitness}_{\text{neighbour}} - \text{Fitness}_{\text{initial}})/\text{Temperature})$.

Step 4: Decrease the temperature.

Step 5: Repeat from step 2 if stop condition is not met.

For the application of optimizing ANN trained on TGA experimentation data, both the inner and outer problem uses a population size of 30 and a maximum generation of 50. This optimization procedure ensures that the optimal thermal conditions of the microalgae can be found together with the recommended catalyst.

3. Results and discussions

3.1 TG-DTG analysis of *C. vulgaris*

The thermal degradation profiles of thermogravimetry (TG) and derivative thermogravimetry (DTG) curves of *C. vulgaris* with and without the presence of HZSM-5 zeolite and limestone catalyst are shown in Fig. 3. The TGA curves were used to analyze the degradation profile of the samples at different temperature stages. Meanwhile, the DTG curves were used to determine the temperature in which the samples undergo the maximum degradation and it was divided into three main volatilization stages namely stage I, stage II and stage III. The first degradation stage (Stage I) of *C. vulgaris* occurred from 50.0 °C to 190.0 °C was due to the intrinsic breakdown of lipids and proteins as well as the removal of moisture in the microalgae cells. Then, the second degradation stage (Stage II) started at 190.0 °C to 600.0 °C (Bach et al., 2017). A significant mass loss of *C. vulgaris* was observed in this stage as it has the highest maximum degradation as shown in the DTG curve. This phenomenon was due to the degradation of the organic compounds in the cell such as protein, carbohydrate and lipids. Lastly, the third degradation stage (Stage III) observed at higher temperature than 600.0 °C. This stage is the final breakdown of lipids which associated with the breakdown of the fatty acid chains (FFA) in the cell (Figueira et al., 2015). The leftover solid residues are the undecomposed ash.

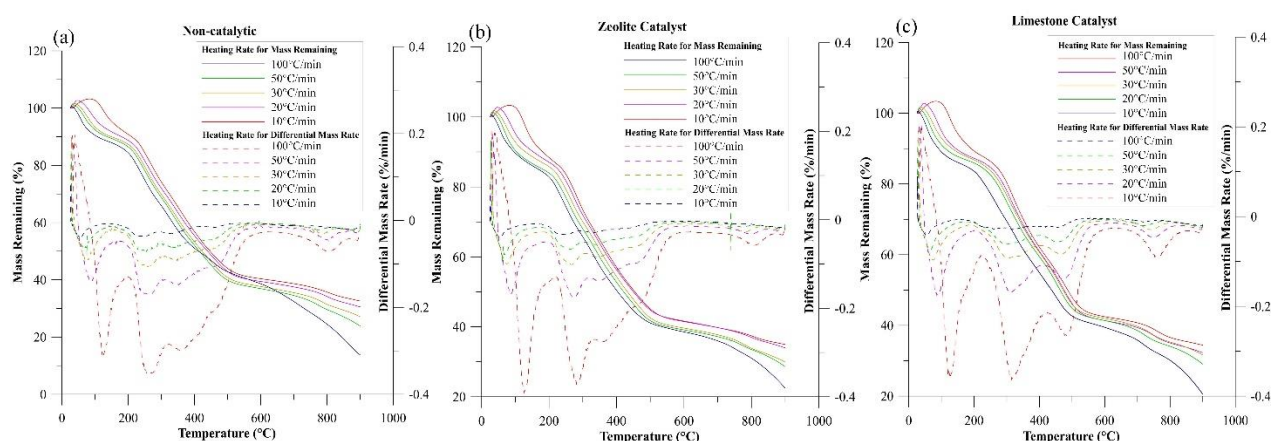


Fig. 3: TGA and DTG curves of (a) non-catalytic degradation of *C. vulgaris*, (b) catalytic degradation of *C. vulgaris* using limestone catalyst, (c) catalytic degradation of *C. vulgaris* using HZSM-5 zeolite.

Table 1 shows the mass loss percentage for both catalytic and non-catalytic thermal degradation at different heating rate ranging from 10.0 °C/min to 100.0 °C/min. Highest average mass loss percentage was obtained in catalytic thermal degradation of *C. vulgaris* using limestone, followed by catalytic thermal degradation of *C. vulgaris* using HZSM-5 zeolite and non-catalytic thermal

degradation of *C. vulgaris*. This phenomenon can be explained through the base catalytic effect of CaO metal oxide element in limestone. Previous study has reported that the addition of base catalyst can improve the quality and yield of the biomass pyrolysis oil. CaO can be used as an absorber or catalyst to enhance the efficiency of the process as well as capture the CO₂ produced and convert it to CaCO₃. This will further reduce the tar formation and enhance the quality of biofuel production by converting long hydrocarbon chains to short hydrocarbon chains fuel (Chen et al., 2019).

Table 1: Mass loss during non-catalytic and catalytic thermal decomposition of *C. vulgaris* using HZSM-5 zeolite and limestone catalyst.

| | Heating Rate (β , °C/min) | T _{initial} (°C) | T _{final} (°C) | T _{max} (°C) | Mass loss (%) |
|--|-------------------------------------|------------------------------|----------------------------|--------------------------|------------------|
| <i>C. vulgaris</i> (without catalyst) | 10 | 140.34 | 553.97 | 247.80 | 86.3 |
| | 20 | 154.59 | 565.64 | 254.70 | 76.11 |
| | 30 | 160.42 | 578.58 | 255.70 | 72.87 |
| | 50 | 173.94 | 596.09 | 268.77 | 69.41 |
| | 100 | 189.60 | 619.41 | 272.54 | 67.42 |
| Average | - | 163.78 | 582.74 | 259.90 | 74.42 |
| <i>C. vulgaris</i> – HZSM-5 zeolite | 10 | 157.94 | 533.10 | 251.93 | 86.68 |
| | 20 | 173.15 | 562.11 | 264.55 | 80.47 |
| | 30 | 183.07 | 596.11 | 266.39 | 79.17 |
| | 50 | 191.96 | 605.09 | 274.52 | 75.17 |
| | 100 | 210.59 | 620.55 | 281.02 | 74.17 |
| Average | - | 183.34 | 583.39 | 267.68 | 79.13 |
| <i>C. vulgaris</i> – Limestone | 10 | 154.05 | 554.05 | 264.49 | 88.58 |
| | 20 | 173.94 | 562.16 | 300.66 | 79.97 |
| | 30 | 178.53 | 576.21 | 307.24 | 77.47 |
| | 50 | 199.23 | 593.39 | 322.59 | 76.87 |
| | 100 | 215.94 | 609.33 | 324.10 | 74.67 |
| Average | - | 184.34 | 579.03 | 303.82 | 79.51 |

3.2 Training and Validation of ANN

The actual optimum conditions of the thermal decomposition process cannot be determined simply based on Fig. 3. Therefore, this work employs the TG data to a neural network and determine the optimal condition by optimizes the outputs of the neural network instead. Using the PDSE algorithm, a total of 30,000 ANN with different activation function and topologies were evaluated. A total of 11 activation functions are considered, which includes softmax, exponential linear unit (elu), scaled exponential linear unit (selu), softplus, softsign, rectified linear unit (ReLU), hyperbolic tangent (tanh), sigmoid, hard sigmoid, exponential (Exp) and linear functions. One of the advantages of the PDSE algorithm is that evolution can easily be parallelized or distributed across multiple computation machines with ease. In this work, the training was distributed over 3 machines with Intel(R) Core (TM) i5-4460, i5-8250 and i7-6700HQ with NVIDIA GeForce GTX 950M. The training time took approximately 12 hours in total. Referring to Fig. 4(a) to 4(c) the PDSE algorithm steadily reduced the loss of the ANN with best neural architecture on extra evaluated ANNs. The algorithm has shown success in achieving optimality within a reasonable context for every single case of catalyst and depth of ANN. This demonstrates the robustness of the algorithm in obtaining an optimal neural architecture.

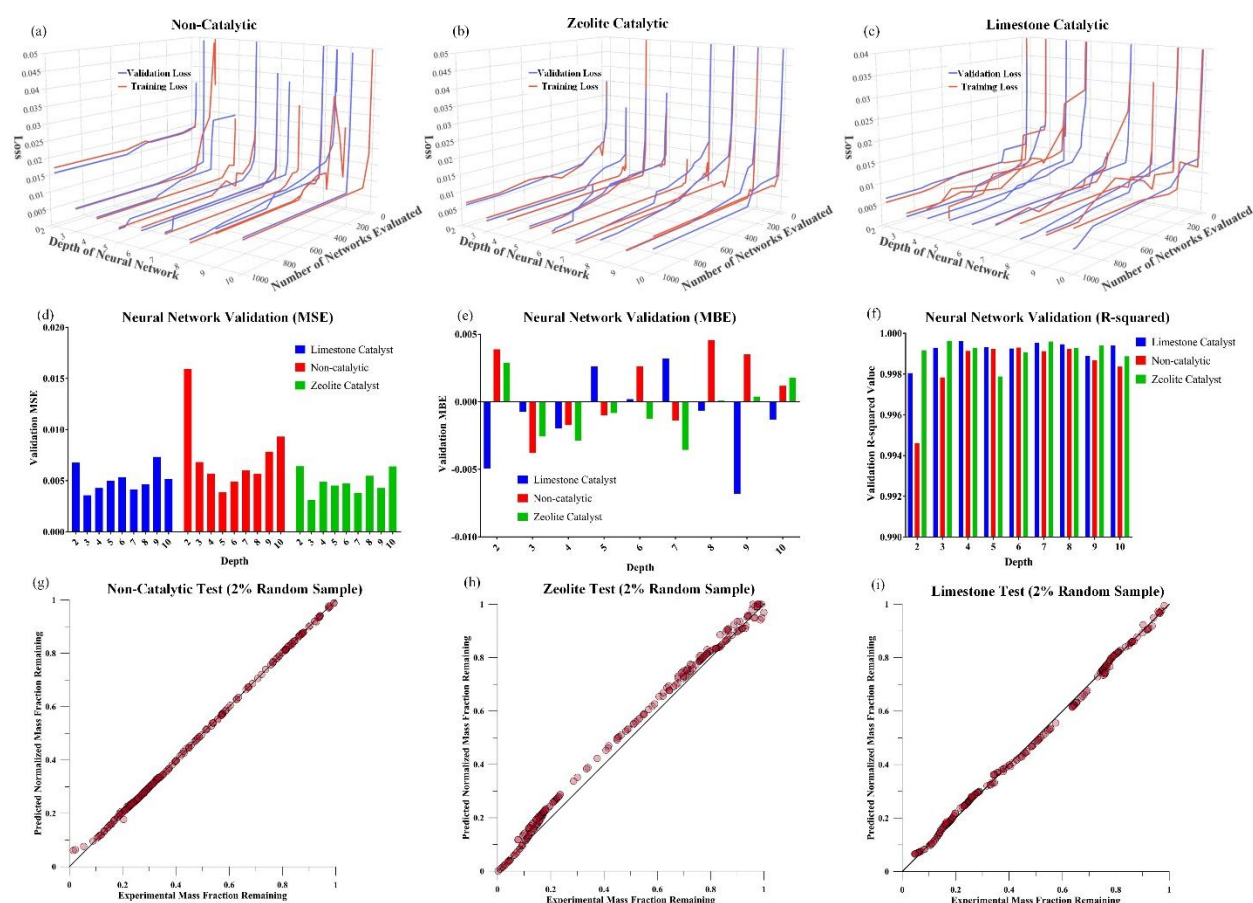


Fig. 4: Training and Validation of ANN (a) non-catalytic degradation of *C. vulgaris*, (b) catalytic degradation of *C. vulgaris* using HZSM-5 zeolite catalyst, (c) catalytic degradation of *C. vulgaris* using limestone catalyst dataset; Accuracy validation of ANN by (d) Mean Squared Error, (e) Mean Bias Error, (f) R-squared value; Predictions against (g) experimental data for non-catalytic testing, (h) experimental data for zeolite testing, (i) experimental for limestone testing.

From Fig. 4(d), it can be observed that there is an overall trend of improvement of loss (MSE) until a specific depth, and then the loss increases giving a “U” shaped trend. This phenomenon is due to the limitations of computational power (costs) in a larger search space as constrained by the maximum search costs in the PDSE algorithm. It is worth mentioning that the maximum search cost is set to reflect an acceptable computation time for the algorithm, and hence it is representative of the machine’s computation power. With a more powerful computational machine, “maximum search cost” within the PDSE algorithm can be improved. Hence, the algorithm can more effectively exploit better architectures of neural network with the same depth. The authors also highlight that the problem of evolving neural networks faces the exploitation-exploration dilemma (Tan et al., 2009) where computation power and time is fixed, and search quality (exploitation) is controlled by “maximum search costs” while search area (exploration) is controlled by the range of network’s depth searched. Nevertheless, referring to Fig. 4(e) and 4(f), the PDSE algorithm has found very convincing neural architecture for all cases and depths with MBE overall between - 0.0050 to 0.0050 and R-squared overall above 0.9950. Note that the predictions made by the model against the experimental data were shown in Figure 4(g) to 4(h).

From Fig. 5, the prediction space of each evolutionary neural network can be observed to be relatively smooth with no sudden disconnections which infer that the networks are well trained with low chance of overfitting. For the experiment of limestone catalyst, PDSE produced a neural network with a depth of 3, having a topology of [173, 81, 1] and activation function of [ReLU, ReLU, Exp]. Non-catalytic experiment required a neural network with deeper depth of 5, topology of [512, 282, 68, 52, 1] and activation function of [tanh, elu, softmax, Relu, Exp]. A very interesting phenomenon in this topology is the evolution of a softmax function which re-normalized the weights in the middle of the neural network, leading to better performances. In the case of HZSM-5 zeolite catalytic experiment, the neural architecture is found to be [348, 214, 1] and activation of [Exp, Linear, Hard Sigmoid].

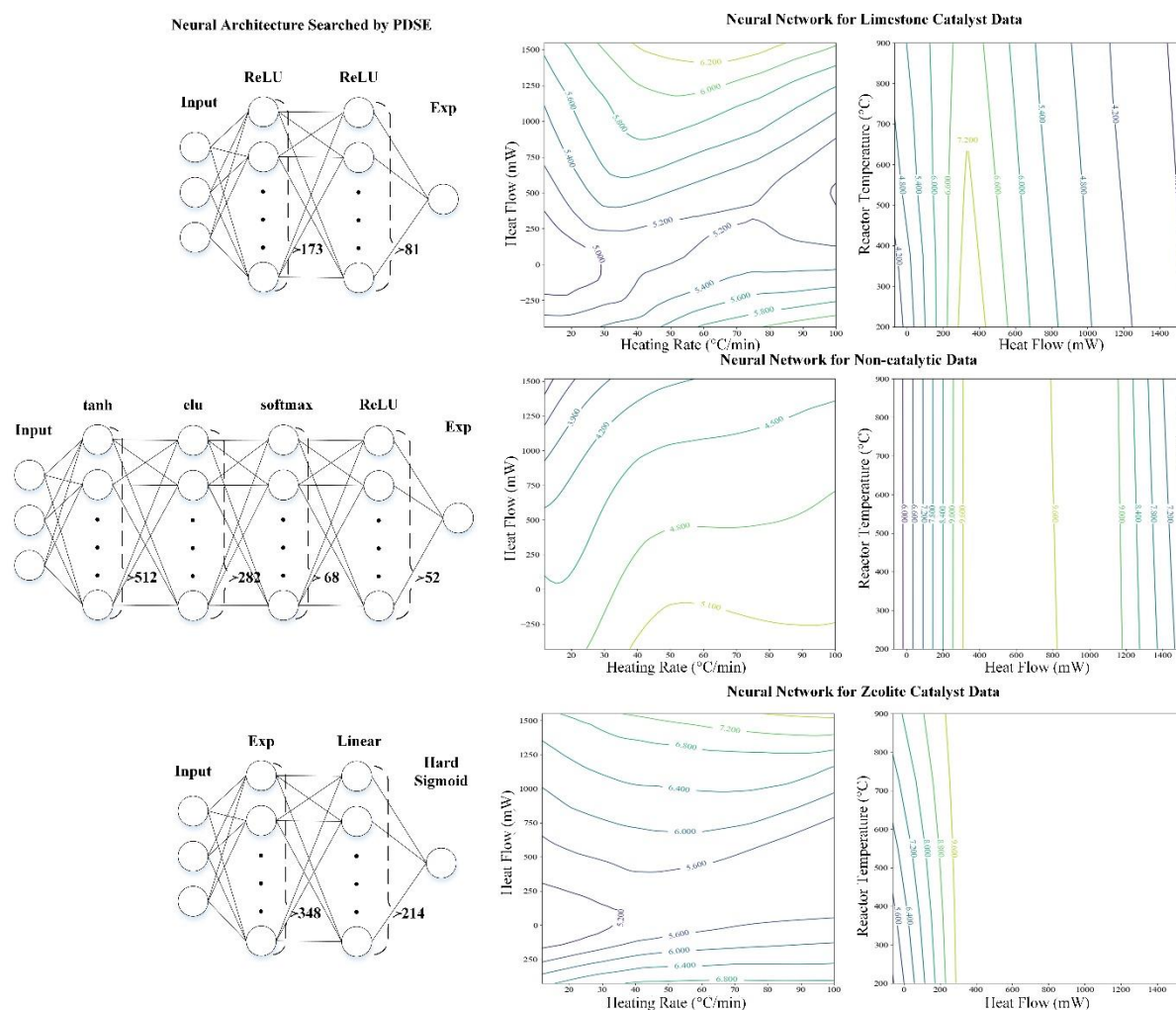


Fig. 5: Neural architecture by PDSE and prediction space (contour represents mass remaining).

The best obtained validation metrics of the trained evolutionary neural networks are tabularized in Table 2. Validation RMSE of all experiments are simultaneously below 0.0075 (i.e., 0.0071 for the case using limestone as catalyst; 0.0075 for the case without using catalyst; 0.0050 for the case using HZSM-5 zeolite catalyst), demonstrating the robustness in the evolutionary neural network model. Furthermore, validation MBE were all smaller than a magnitude of 0.0026 (i.e., -0.0007 for the case using limestone as catalyst; -0.0010 for the case without using catalyst; -0.0026 for the case using HZSM-5 zeolite catalyst), this shows that the model is not biased towards a certain effect of association. It is also worth pointing out that the R^2 metric does not reflect the real performance of models when the values of two models are close (e.g. 0.9991 and 0.9996). A popular example to demonstrate this is when the predicted value is a dataset of [3,4,5] and actual values are [1,2,3], the R^2 value is 1.0 but the average error is 2. Alexander et al. (2015) also observed this phenomenon and encouraged the use of error metrics over R^2 . Nevertheless, all models obtained validation R^2 value above 0.9990 (i.e., 0.9993 for the case using limestone as catalyst; 0.9992 for the case without using catalyst; 0.9996 for the case using HZSM-5 zeolite catalyst).

To underline the performance of evolutionary neural networks within the TGA modelling ecosystem, we state the performances of the models within some related works. Firstly, a recent work from Xie et al. (2018) tested Radial Basis Function Network (RBFN) and Bayesian Regularized Network (BRN) modelling on the thermal analysis of textile dyeing sludge and pomelo peel. In the work, RBFN attained 0.8506 RMSE and 0.9989 R² while BRN attained 0.3277 RMSE and 0.9989 R². Buyukada (2016) also used Multi-Layered Perceptrons (MLP) to model TGA analysis of peanut hull and coal blend, giving a result of 1.5678 RMSE, 0.0501 MBE and 0.9999 R². For the feedstock of hazelnut husks and lignite coal, Yıldız et al. (2016) also obtained a result of 0.6240 RMSE, 0.4840 MBE and 0.9994 R² using MLP model. It is also worth pointing out that previous works related to the modelling of *C. Vulgaris* attained 0.9000 to 0.9800 regression R² values using Kissinger-Akahira-Sunose (KAS) model and 0.9180 to 0.9490 regression R² values using Flynn-Wall-Ozawa (FWO) model (Figueira et al., 2015). Considering a mixed feedstock of *C. Vulgaris*, wood and polypropylene, Azizi et al. (2017) obtained 0.6899 to 0.9906 regression R² values with KAS model and 0.7336 to 0.9910 regression R² values with FWO model. All previous work stated had provided admirable contribution to the fields of thermogravimetric analysis and can be considered as the current state-of-art. Contrarily, it is clear that our modelling technique achieved results with two order of magnitude better in RMSE and at least one order of magnitude better in MBE than the current state-of-art results.

3.3 Optimized results using Simulated Annealing method

The bi-level optimization by Simulated Annealing to find an optimum thermal condition for the conversion of *C. vulgaris* took 27 minutes on a machine with Intel(R) Core(TM) i5-8250. In general, the Simulated Annealing algorithm performs well with increasing fitness on new generations within the algorithm. Fig. 6(a) is taken as an example (temperature range from 700.0 °C to 750.0 °C), the averaged fitness within the population was also steadily increasing, showing that searching agents within the population are gradually improving their search solution on average. The optimum conditions were found in generation 41. However, the algorithm was allowed to run until generation 100 for confirmation of optimality. At higher number of generations, the mass remaining fraction was already quite stable, attaining good values below 0.2. For other temperature ranges, very similar phenomena were observed, and authors think it is trivial to present similar figures. Overall, the Simulated Annealing algorithm shows good improvement of mass remaining (in mass fraction), while consistently have its population of searchers move to a better solution on average. This shows that an optimal point is statistically guaranteed to be found.

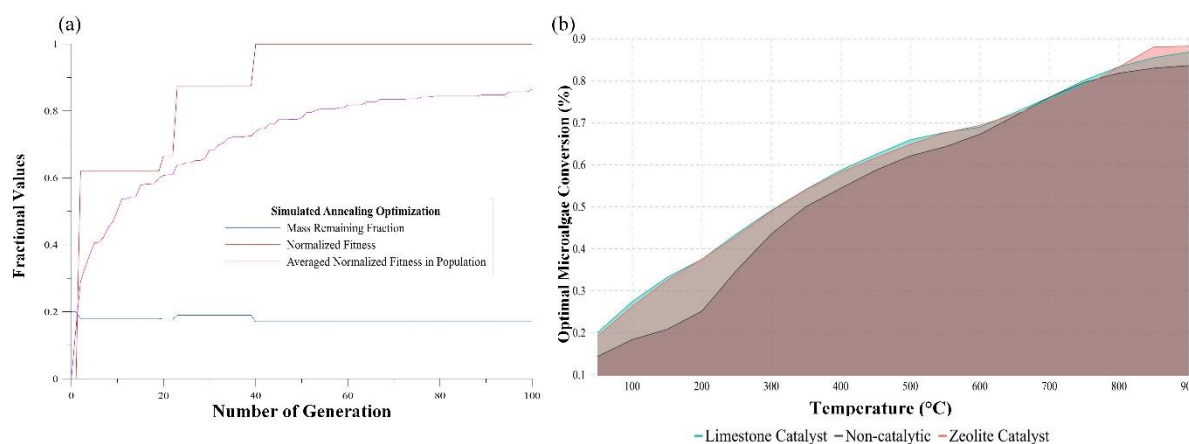


Fig. 6: Optimization by simulated annealing (a) example of convergence curve at 700°C to 750 °C, (b) optimal conversion against reactor temperature.

Referring to the Pareto curve shown in Fig. 6(b), each point of the curve is the local optimal of conversion under a specified temperature; while the one with the highest conversion is denoted as global optimal under a specified temperature. At temperatures below 550.0 °C, limestone catalyst showed a significant improvement on the *C. vulgaris* conversion. This is due to the alkali CaO element in limestone catalyst which reduced the activation energy of the pyrolysis reaction and resulting in a higher conversion of *C. vulgaris*. For this temperature range, the limestone catalyst results in higher conversion than HZSM-5 zeolite catalyst converting almost all the carbohydrates, protein and lipid to bio-oil. Meanwhile at temperatures between 550.0 °C to 800.0 °C, both limestone and HZSM-5 zeolite catalysts shown almost similar catalytic effect in converting the *C. vulgaris* as shown in Table 3. Previous study has reported that Brønsted acid sites predominate in HZSM-5 zeolites will be activated at temperature above 500.0 °C and this could further enhance the secondary tar cracking such as dehydrogenation, decarboxylation, and aromatization to convert the light vapors and tar to form water, carbon dioxide, carbon monoxide, alkanes, alkene, methane and hydrogen (Vitolo et al., 2001). Thus, higher gaseous yield will be obtained in this stage. At temperature above 800.0 °C, the limestone catalyst started to lose its stability and catalytic activity due to the degradation of CaO to CO₂. Thus, HZSM-5 zeolite is a more suitable catalyst in thermal degradation process at temperature above 800.0 °C.

Table 2: Optimum conditions to enhance *C. vulgaris* conversion at different temperature range.

| Temperature Range (°C) | Optimal Heating Rate (°C/min) | Optimal Heating Flow (mW) | Optimal Temperature (°C) | Best Catalyst | Microalgae Conversion (%) |
|------------------------|-------------------------------|---------------------------|--------------------------|---------------|---------------------------|
| 30 - 50 | 5.0 | 300.0 | 50 | Limestone | 20.0 |
| 50 - 100 | 5.0 | 300.0 | 100 | Limestone | 27.4 |
| 100 - 150 | 5.0 | 300.0 | 150 | Limestone | 33.1 |

| | | | | | |
|-----------|------|-------|-----|------------------|------|
| 150 - 200 | 5.0 | 300.0 | 200 | Limestone | 37.5 |
| 200 - 250 | 5.0 | 300.0 | 250 | Limestone | 43.6 |
| 250 - 300 | 5.0 | 278.4 | 300 | Limestone | 49.2 |
| 300 - 350 | 5.0 | 76.1 | 350 | Limestone | 54.2 |
| 350 - 400 | 5.0 | 59.1 | 400 | Limestone | 58.7 |
| 400 - 450 | 15.8 | 0.0 | 450 | Limestone | 62.5 |
| 450 - 500 | 20.2 | 0.0 | 500 | Limestone | 64.9 |
| 500 - 550 | 19.9 | 0.0 | 550 | Limestone | 67.7 |
| 550 - 600 | 5.0 | 174.8 | 600 | HZSM-5 Zeolite | 69.4 |
| 600 - 650 | 5.0 | 0.0 | 650 | HZSM-5 Zeolite | 72.0 |
| 650 - 700 | 5.0 | 0.0 | 700 | Limestone | 76.1 |
| | 5.0 | 300.0 | 700 | Non-Catalytic* | 76.1 |
| | 5.0 | 0.0 | 700 | HZSM-5 Zeolite** | 75.0 |
| 700 - 750 | 5.0 | 0.0 | 750 | Limestone | 80.1 |
| | 5.0 | 300.0 | 750 | Non-Catalytic** | 79.6 |
| | 5.0 | 0.0 | 750 | HZSM-5 Zeolite** | 78.6 |
| 750 - 800 | 5.0 | 0.0 | 800 | Limestone | 83.3 |
| | 5.0 | 300.0 | 800 | Non-Catalytic** | 81.8 |
| | 5.0 | 0.0 | 800 | HZSM-5 Zeolite** | 83.3 |
| 800 - 850 | 5.0 | 0.0 | 850 | HZSM-5 Zeolite | 88.0 |
| 850 - 900 | 5.0 | 0.0 | 900 | HZSM-5 Zeolite | 88.3 |

*Non-catalytic can reach maximum conversion, but more heating flow is required. This is not the bi-level optimum, however, authors decide to present it.

**Near to optimum points that can be considered.

4. Conclusion

Thermal conversion of *C. vulgaris* was successfully modeled using neuro-evolutionary approach. Based on the benchmarking results, the simulation performance of the proposed approach significantly outperforms other conventional methods with lower RMSE and MBE values (> 90 % lesser error) compared to other methods; while maintaining a high R^2 value (> 0.9990). A bi-level optimization was performed using Simulated Annealing algorithm to determine the optimal operating conditions. The highest conversion of *C. vulgaris* (88.3 %) to bio-oil and gaseous product was achieved at a temperature of 900.0 °C, heating rate of 5.0 °C/min, and with the presence of HZSM-5 zeolite catalyst.

Acknowledgement

The authors would like to acknowledge financial support from the Ministry of Education, Youth and Sports of the Czech Republic under OP RDE [grant number CZ.02.1.01/0.0/0.0/16_026/0008413] “Strategic Partnership for Environmental Technologies and Energy Production”.

Declaration of interest

Declarations of interest: none

References

1. Abbas, T., Awais, M.M., Lockwood, F.C., 2003. An artificial intelligence treatment of devolatilization for pulverized coal and biomass in co-fired flames. *Combust Flame* 132(3), 305-318. doi.org/10.1016/S0010-2180(02)00482-0
2. Adenle, A.A., Haslam, G.E., Lee, L., 2013. Global assessment of research and development for algae biofuel production and its potential role for sustainable development in developing countries. *Energ Policy* 61, 182-195. doi.org/10.1016/j.enpol.2013.05.088
3. Alexander, D.L., Tropsha, A. and Winkler, D.A., 2015. Beware of R 2: simple, unambiguous assessment of the prediction accuracy of QSAR and QSPR models. *J Chem Inf Model* 55(7), 1316-1322. doi.org/10.1021/acs.jcim.5b00206
4. Azizi, K., Moraveji, M.K., Najafabadi, H.A., 2017. Characteristics and kinetics study of simultaneous pyrolysis of microalgae *Chlorella vulgaris*, wood and polypropylene through TGA. *Bioresource Technol* 243, 481-491. doi.org/10.1016/j.biortech.2017.06.155
5. Bach, Q.V., Chen, W.H., 2017. Pyrolysis characteristics and kinetics of microalgae via thermogravimetric analysis (TGA): A state-of-the-art review. *Bioresource Technol* 246, 88-100. doi.org/10.1016/j.biortech.2017.06.087
6. Barnard, J.A., Hughes, H.W.D., 1960. The pyrolysis of ethanol. *T Faraday Soc* 56, 55-63.
7. Buyukada, M., 2016. Co-combustion of peanut hull and coal blends: Artificial neural networks modeling, particle swarm optimization and Monte Carlo simulation. *Bioresource Technol* 216, 280-286. doi.org/10.1016/j.biortech.2016.05.091
8. Carlson, T.R., Jae, J., Lin, Y.-C., Tompsett, G.A., Huber, G.W., 2010. Catalytic fast pyrolysis of glucose with HZSM-5: The combined homogeneous and heterogeneous reactions. *J Catal* 270(1), 110-124. doi.org/10.1016/j.jcat.2009.12.013

9. Chan, Y.H., Cheah, K.W., How, B.S., Loy, A.C.M., Shahbaz, M., Singh, H.K.G., Yusuf, N.R., Ahmad Shuhaili, A.F., Yusup, S., Ghani, W.A.W.A.K., Rambli, J., Kansha, Y., Lam, H.L., Hong, B.H., Ngan, S.L., 2019. An overview of biomass thermochemical conversion technologies in Malaysia. *Sci Total Environ* 680, 105-123. doi.org/10.1016/j.scitotenv.2019.04.211
10. Chen, X., Li, S., Liu, Z., Chen, Y., Yang, H., Wang, X., Che, Q., Chen, W., Chen, H., 2019. Pyrolysis characteristics of lignocellulosic biomass components in the presence of CaO. *Bioresource Technol* 287, 121493. doi.org/10.1016/j.biortech.2019.121493
11. Conesa, J.A., Caballero, J.A., Reyes-Labarta, J.A., 2004. Artificial neural network for modelling thermal decompositions. *J Anal Appl Pyrol* 71(1), 343-352. doi.org/10.1016/S0165-2370(03)00093-7
12. Costa, J.A.V., Morais, M.G., 2011. The role of biochemical engineering in the production of biofuels from microalgae, *Bioresource Technol* 102(1), 2-9. doi.org/10.1016/j.biortech.2010.06.014
13. Ding, S., Li, H., Su, C., Yu, J., Jin, F., 2011. Evolutionary artificial neural networks: a review. *Artif Intell Rev* 39(3), 251-260. doi.org/10.1007/s10462-011-9270-6
14. Fazilat, H., Akhlaghi, S., Shiri, M.E., Sharif, A., 2012. Predicting thermal degradation kinetics of nylon6/feather keratin blends using artificial intelligence techniques. *Polymer* 53(11), 2255-2264. doi.org/10.1016/j.polymer.2012.03.053
15. Figueira, C.E., Moreira Jr, P.F., Giudici, R., 2015. Thermogravimetric analysis of the gasification of microalgae *Chlorella vulgaris*. *Bioresource Technol* 198, 717-724. doi.org/10.1016/j.biortech.2015.09.059
16. Fister Jr, I., Yang, X.S., Fister, I., Brest, J. and Fister, D., 2013. A brief review of nature-inspired algorithms for optimization. arXiv preprint arXiv:1307.4186.
17. Floreano, D., Dürr, P., Mattiussi, C., 2008. Neuroevolution: from architectures to learning. *Evol Intell* 1(1), 47-62. doi.org/10.1007/s12065-007-0002-4
18. Gai, C., Zhang, Y., Chen, W.-T., Zhang, P., Dong, Y., 2013. Thermogravimetric and kinetic analysis of thermal decomposition characteristics of low-lipid microalgae. *Bioresource Technol* 150, 139-148. doi.org/10.1016/j.biortech.2013.09.137
19. Gan, D.K.W., Loy, A.C.M., Chin, B.L.F., Yusup, S., Unrean, P., Rianawati, E., Acda, M.N., 2018. Kinetics and thermodynamic analysis in one-pot pyrolysis of rice hull using renewable calcium oxide based catalysts. *Bioresource Technol* 265, 180-190. doi.org/10.1016/j.biortech.2018.06.003
20. Goffe, W.L., Ferrier, G.D., Rogers, J., 1994. Global optimization of statistical functions with simulated annealing. *J Econometrics* 60(1-2), 65-99. doi.org/10.1016/0304-4076(94)90038-8
21. International Energy Agency (IEA), 2019. Global energy demand rose by 2.3% in 2018, its fastest pace in the last decade. <https://www.iea.org/newsroom/news/2019/march/global-energy-demand-rose-by-23-in-2018-its-fastest-pace-in-the-last-decade.html> (accessed June 17, 2019).
22. Jaderberg, M., Dalibard, V., Osindero, S., Czarnecki, W.M., Donahue, J., Razavi, A., Vinyals, O., Green, T., Dunning, I., Simonyan, K. and Fernando, C., 2017. Population based training of neural networks. arXiv preprint arXiv:1711.09846.

23. Kim, S.-S., Ly, H.V., Choi, G.-H., Kim, J., Woo, H.C., 2012. Pyrolysis characteristics and kinetics of the alga *Saccharina japonica*. *Bioresource Technol* 123, 445-451. doi.org/10.1016/j.biortech.2012.07.097
24. Kingma, D.P., Ba, J., 2014. Adam: A method for stochastic optimization. arXiv preprint arXiv:1412.6980.
25. Mata, T.M., Martins, A.A., Caetano, N.S., 2010. Microalgae for biodiesel production and other applications: A review. *Renew Sust Energ Rev* 14(1): 217-232. doi.org/10.1016/j.rser.2009.07.020
26. Mayol, A., Maningo, J., Chua-Unsu, A., Felix, C., Rico, P., Chua, G., Manalili, E., Fernandez, D., Cuello, J., Bandala, A., Ubando, A., Madrazo, C., Dadios, E. and Culaba, A., 2018. Application of Artificial Neural Networks in prediction of pyrolysis behavior for algal mat (LABLAB) biomass. In 2018 IEEE 10th International Conference on Humanoid, Nanotechnology, Information Technology, Communication and Control, Environment and Management (HNICEM). IEEE, Baguio City, Philippines. doi.org/10.1109/HNICEM.2018.8666376
27. Metropolis, N., Rosenbluth, A.W., Rosenbluth, M.N., Teller, A.H. and Teller, E., 1953. Equation of state calculations by fast computing machines. *J Chem Phys* 21(6), 1087-1092. doi.org/10.1063/1.1699114
28. Mettler, M.S., Paulsen, A.D., Vlachos, D.G., Dauenhauer, P.J., 2014. Tuning cellulose pyrolysis chemistry: selective decarbonylation via catalyst-impregnated pyrolysis. *Catal Sci Technol* 4, 3822-3825. doi.org/10.1039/C4CY00676C
29. Mhaskar, H.N., Poggio, T., 2016. Deep vs. shallow networks: An approximation theory perspective. *Analy Appl* 14(6), 829-848. doi.org/10.1142/S0219530516400042
30. Milano, J., Ong, H.C., Masjuki, H.H., Chong, W.T., Lam, M.K., Loh, P.K., Vellayan, V., 2016. Microalgae biofuels as an alternative to fossil fuel for power generation. *Renew Sust Energ Rev* 58, 180-197. doi.org/10.1016/j.rser.2015.12.150
31. Mohr, A., Raman, S., 2013. Lessons from first generation biofuels and implications for the sustainability appraisal of second generation biofuels. *Energ Policy* 63, 114-122. doi./10.1016/j.enpol.2013.08.033
32. Naqvi, S.R., Tariq, R., Hameed, Z., Ali, I., Taqvi, S.A., Naqvi, M., Niazi, M.B.K., Noor, T., Farooq, W., 2018. Pyrolysis of high-ash sewage sludge: Thermo-kinetic study using TGA and artificial neural networks. *Fuel* 233, 529-538. doi.org/10.1016/j.fuel.2018.06.089
33. Organization of the Petroleum Exporting Countries (OPEC), 2019. OPEC: energy, climate change and sustainable development. https://www.opec.org/opec_web/static_files_project/media/downloads/publications/OB042019.pdf (accessed June 19, 2019).
34. Raymundo, L.M., Mullen, C.A., Strahan, G.D., Boateng, A.A., Trierweiler, J.O., 2019. Deoxygenation of Biomass Pyrolysis Vapors via in Situ and ex Situ Thermal and Biochar Promoted Upgrading. *Energ Fuels* 33(3), 2197-2207. doi.org/10.1021/acs.energyfuels.8b03281
35. Salimans, T., Ho, J., Chen, X., Sidor, S. and Sutskever, I., 2017. Evolution strategies as a scalable alternative to reinforcement learning. arXiv preprint arXiv:1703.03864.
36. Shi, Y., Eberhart, R., 1998. A modified particle swarm optimizer. In 1998 IEEE international conference on evolutionary computation proceedings. In 1998 IEEE International Conference

- on Evolutionary Computation Proceedings. IEEE World Congress on Computational Intelligence (Cat. No.98TH8360). IEEE, Anchorage, USA. doi.org/10.1109/ICEC.1998.699146
37. Stanley, K.O., Clune, J., Lehman, J., Miikkulainen, R., 2019. Designing neural networks through neuroevolution. *Nat Mach Intell* 1(1), 24-35. doi.org/10.1038/s42256-018-0006-z
 38. Stanley, K.O., Miikkulainen, R., 2002. Evolving neural networks through augmenting topologies. *Evol Comput* 10(2), 99-127. doi.org/10.1162/106365602320169811
 39. Sun, J., Xiong, X., Wang, M., Du, H., Li, J., Zhou, D., Zuo, J., 2019. Microalgae biodiesel production in China: A preliminary economic analysis. *Renew Sust Energ Rev* 104, 296-306. doi.org/10.1016/j.rser.2019.01.021
 40. Tan, K.C., Chiam, S.C., Mamun, A.A., Goh, C.K., 2009. Balancing exploration and exploitation with adaptive variation for evolutionary multi-objective optimization. *Eur J Oper Res* 197(2), 701-713. doi.org/10.1016/j.ejor.2008.07.025
 41. Teng, S.Y., 2019. tseyet12/EvoOpt: EvoOpt v0.12 pre-release. doi.org/10.5281/zenodo.3241951
 42. Vitolo, S., Bresci, B., Seggiani, M., Gallo, M.G., 2001. Catalytic upgrading of pyrolytic oils over HZSM-5 zeolite: behaviour of the catalyst when used in repeated upgrading–regenerating cycles. *Fuel* 80(1), 17-26. doi.org/10.1016/S0016-2361(00)00063-6
 43. Xie, C., Liu, J., Zhang, X., Xie, W., Sun, J., Chang, K., Kuo, J., Xie, W., Liu, C., Sun, S., Buyukada, M., 2018. Co-combustion thermal conversion characteristics of textile dyeing sludge and pomelo peel using TGA and artificial neural networks. *Appl Energ* 212, 786-795. doi.org/10.1016/j.apenergy.2017.12.084
 44. Yang, H., Norinaga, K., Li, J., Zhu, W., Wang, H., 2018. Effects of HZSM-5 on volatile products obtained from the fast pyrolysis of lignin and model compounds. *Fuel Process Technol* 181, 207-214. doi.org/10.1016/j.fuproc.2018.09.022
 45. Yıldız, Z., Uzun, H., Ceylan, S., Topcu, Y., 2016. Application of artificial neural networks to co-combustion of hazelnut husk–lignite coal blends. *Bioresource Technol* 200, 42-47. doi.org/10.1016/j.biortech.2015.09.114
 46. Zainan, N.H., Srivatsa, S.C., Li, F., Bhattacharya, S., 2018. Quality of bio-oil from catalytic pyrolysis of microalgae *Chlorella vulgaris*. *Fuel* 223, 12-19. doi.org/10.1016/j.fuel.2018.02.166
 47. Zhang, X., Li, C., Tian, A., Guo, Q., Huang, K., 2019. Influence of CaO and HZSM-5 on oxygen migration in *Chlorella vulgaris* polysaccharide pyrolysis. *Carbon Resources Conversion*, 2(2), 111-116. doi.org/10.1016/j.crcon.2019.05.00